

## Magnetic fields in cometary globules – II. CG 30–31 complex

H. C. Bhatt<sup>★</sup>

*Indian Institute of Astrophysics, Bangalore 560 034, India*

Accepted 1999 March 23. Received 1999 February 22; in original form 1998 November 26

### ABSTRACT

Optical linear polarization measurements of stars in the region of the cometary globules CG 30–31 in Vela–Puppis are presented. A polarization map representing the geometry of the magnetic field in the cometary globule complex is produced. The magnetic field is found to be nearly perpendicular to the cometary tails. This is unlike the case of the cometary globule CG 22 in which the field had earlier been found to be aligned with the tail. The observed field direction is more or less parallel to the bipolar molecular outflow from the young stellar object IRS 4 embedded in the head of CG 30.

**Key words:** polarization – ISM: globules – ISM: individual: CG 30–31 complex – ISM: magnetic fields.

### 1 INTRODUCTION

Cometary globules (CGs) are interstellar clouds that show a head–tail morphology similar to the comets. The heads are compact and bright-rimmed. They are completely opaque so that no background stars are seen through them. A faintly luminous tail extending from the head generally points away from a nearby bright early-type star. Systems of CGs have been found in a number of star-forming regions with massive OB type stars (e.g. Hawarden & Brand 1976; Sandqvist 1976; Schneps, Ho & Barret 1980; Zealey et al. 1983; Reipurth 1983; Gyulbudagyan 1985; Sugitani, Fukui & Ogura 1991; Block 1992). The largest of these is the system of  $\sim 30$  CGs in the Vela–Puppis region of the southern sky (Zealey et al. 1983). The tails of the CGs of this system point toward the centre of the large (angular radius  $\sim 18^\circ$ ) region of H $\alpha$  emission nebula called the Gum Nebula (Gum 1952; Zealey et al. 1983). The CGs appear in projection to lie in a ring of angular radius  $\sim 10^\circ$  that encircles the Vela OB2 association (Brandt et al. 1971). The luminous stars  $\zeta$  Puppis (O4f) and  $\gamma^2$  Velorum (WC8 + O9I) and the young Vela pulsar and supernova remnant are seen projected upon the central region.  $\zeta$  Puppis and  $\gamma^2$  Velorum are likely to be members of the Vela OB2 association, the distance of which, from *Hipparcos* parallax measurements, has been found to be  $415 \pm 10$  pc (de Zeeuw et al. 1997; Schaerer, Schmutz & Grenon 1997). Coincident with the ring of the cometary globules, surrounding the Vela OB2 association, there exists an infrared emitting dusty shell as seen in the *IRAS* maps (Sahu 1992). A study (Sridharan 1992) of the kinematics of the CGs suggests that the system of CGs is expanding from the common centre with an expansion velocity of  $\sim 12$  km s $^{-1}$ .

Scenarios for the formation of the cometary globules in the Gum–Vela complex have been suggested by Zealey et al. (1983)

and Reipurth (1983). Relatively smaller dense cloud cores distributed in the parent giant molecular cloud, exposed to the radiation and stellar winds from massive O-type stars in the central OB association, can develop cometary head–tail morphology as the less dense outer parts of the cloud are separated from the core and the dense core is shock-compressed to produce the head. At present  $\zeta$  Puppis is the primary source of radiation responsible for the illumination of the bright-rimmed heads and luminous tails of the CGs in this region. Radiation-driven implosion (RDI) models for the formation and evolution of CGs have been discussed by Bertoldi (1989), Bertoldi & McKee (1990) and Lefloch & Lazareff (1994, 1995). The shock generated by RDI can trigger star formation in the CG heads for which there is considerable evidence (Reipurth 1983; Brand et al. 1983; Pettersson 1984; Bhatt 1993).

It is generally well recognized that magnetic fields play an important role in controlling the morphology of interstellar clouds, their support against collapse or dispersal and the details of the star formation process. What role does the magnetic field play in the structure and evolution of the CGs? Does a magnetic field aligned along the CG tail help confine the gas which, given the observed velocity dispersions, should disperse perpendicular to the tail? The CGs in the Vela–Puppis region provide an interesting variety of structures, physical conditions and geometrical configurations with which to study the effects of the magnetic field (Sridharan, Bhatt & Rajagopal 1996 – Paper I). We began, in 1995, a programme to map the magnetic fields in the Vela–Puppis CGs by making optical linear polarization measurements of stars projected in the regions of these globules. Measurements for CG 22 were presented in Paper I. A majority of the stars seen projected within the cloud boundaries were found to be polarized ( $\sim 1$  per cent) with the electric vector oriented parallel to the CG tail. If the polarization is a result of non-spherical dust grains aligned by the magnetic field (Davis–Greenstein mechanism), then the results for CG 22 imply that the magnetic field in this CG

<sup>★</sup>E-mail: hcbhatt@iiap.ernet.in

is parallel to its tail. Such a magnetic field can help confine the long narrow tail against dispersal in the perpendicular direction because of the observed large velocity dispersion. Is the magnetic field similarly oriented, with respect to the tail direction, in all the cometary globules? Observations of other CGs in different parts of the Vela–Puppis region are required to answer this question. In this paper we present the results of polarization measurements of stars in the region of the CG 30–31 complex that lies about  $4.5^\circ$  south-west of CG 22.

## 2 THE CG 30–31 COMPLEX

CGs 30 and 31 are part of a complex of globules including CG 38. CG 31 itself has several heads (CG 31 A, B, C, D, E) and the tails merge into a dark cloud  $\sim 25$  arcmin behind CG 30 (Reipurth 1983). In contrast with the sharply defined, long ( $\sim 75$  arcmin) tail of CG 22, the tails associated with CGs 30 and 31 are shorter ( $\sim 25$  arcmin) and amorphous.

CG 30 shows signs of recent star formation. Embedded in its head is the infrared source CG 30-IRS 4 (IRAS 08076-3556) exciting the Herbig–Harro object HH 120 (Pettersson 1984) and illuminating the small optical nebulosity R 2 (Reipurth 1981). Imaging polarimetry of the optical nebulosity R 2 in CG 30 by Scarrott et al. (1990) suggested that the outflow activity from the embedded source excavated a cavity in the cloud and the optical nebulosity is produced as the walls of the cavity are illuminated by radiation from the central star that is otherwise hidden from direct view in the optical. A dense molecular outflow originating from CG 30-IRS 4 has indeed been detected in CO line observations by Nielsen et al. (1998).

## 3 OBSERVATIONS

Linear polarization measurements were made with a fast star-and-sky chopping polarimeter (Jain & Srinivasulu 1991) coupled at the  $f/13$  Cassegrain focus of the 1-m telescope at the Vainu Bappu Observatory, Kavalur of the Indian Institute of Astrophysics. An unfiltered dry-ice cooled R943-02 Hamamatsu photomultiplier tube was used as the detector. An aperture of 15 arcsec was used for all the observations, which were made on the nights of 1997 March 7 and 8. The instrumental polarization was determined by observing unpolarized standard stars from Serkowski (1974). It was found to be  $\sim 0.1$  per cent, and has been subtracted vectorially from the observed polarization of the programme stars. The zero of the polarization position angle was determined by observing the polarized standards from Hsu & Breger (1982). In all, 16 stars in different regions of CG 30–31 were measured. Fig. 1, reproduced from the Digitized Sky Survey (DSS), shows the region of the cometary globules observed.

## 4 RESULTS

The results of our polarization measurements are presented in Table 1. The stars observed have been numbered as shown in Fig. 1. Stars 1, 5 and 6 are identified with SAO 198864, 198868 and 198851 respectively. Table 1 gives the measured polarization  $P$  (in per cent), the position angle (of the  $E$  vector)  $\theta$  (in degrees) and the probable errors  $\epsilon_P$  and  $\epsilon_\theta$  associated with  $P$  and  $\theta$ . The position angles listed are measured from north, increasing eastward. As a rough guide to the brightness of the stars measured, column 1 of Table 1 gives the magnitudes of the stars

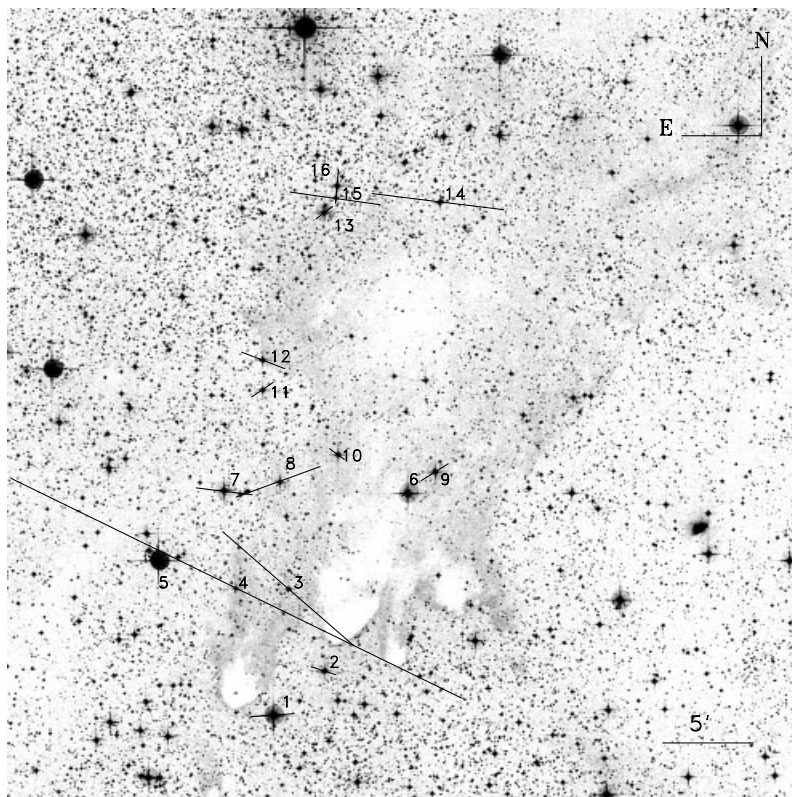


**Figure 1.** Polarization map for the region of the CG 30–31 complex. The polarization vectors have been drawn centred on the stars observed. The optical image has been reproduced from the Digitized Sky Survey. The angular scale is indicated by the horizontal bar drawn near the lower right corner.

**Table 1.** Polarization measurements of stars in the region of CG 30–31.

Star No.	mag.	$P$ (per cent)	$\epsilon_P$ (per cent)	$\theta$ ( $^\circ$ )	$\epsilon_\theta$ ( $^\circ$ )
1 (SAO 198864)	9.1	0.34	0.06	94	5
2	10.2	0.20	0.09	72	13
3	12.2	1.36	0.23	49	5
4	12.8	3.94	0.04	64	1
5 (SAO 198868)	7.4	0.17	0.12	61	20
6 (SAO 198851)	8.8	0.08	0.06	129	21
7	9.1	0.44	0.07	83	5
8	11.0	0.70	0.11	110	5
9	9.4	0.25	0.06	122	7
10	10.4	0.14	0.09	54	18
11	11.4	0.20	0.17	124	24
12	9.5	0.36	0.07	69	6
13	10.1	0.16	0.08	127	14
14	10.5	1.04	0.18	83	5
15	10.8	0.71	0.14	82	6
16	11.8	0.26	0.24	175	26

obtained from the mean intensity. The photocathode response may be considered to approximate the Johnson  $R$  band. Probable errors in these magnitudes are  $\sim 0.5$  mag. Superposed on the optical image of the CG 30–31 region, a polarization map is also shown in Fig. 1. Centred on the stars observed, the polarization vectors have been drawn. The length of the polarization vector is proportional to the percentage polarization  $P$  and it is oriented parallel to the direction indicated by  $\theta$ .

## 5 DISCUSSION

It can be seen from Table 1 that the observed polarization of stars in the region of CG 30–31 ranges from  $\sim 0.1$  to  $\sim 4$  per cent. Stars 1, 2, 5 and 11, which are seen projected outside the nebular boundaries of the cloud (Fig. 1), show relatively lower values ( $\leq 0.34$  per cent) of polarization. Stars seen projected within the cloud boundaries and that have fainter apparent magnitudes show relatively larger values of polarization, while the brighter stars tend to show lower values of polarization. We have very little information on the distances of individual stars, but as will be argued below, the brighter stars projected within the cloud boundaries and showing lower values of polarization are likely to be foreground stars. The polarization observations suggest that the dust in the cloud is causing extinction and polarization of the fainter stars seen through the cloud.

The histogram in Fig. 2 shows the distribution of the observed polarization position angles. Fig. 2 is also a plot of the observed percentage polarization against the position angle. The position angles range from  $\sim 50^\circ$  to  $\sim 130^\circ$ . Star 16, showing a small polarization with large uncertainty ( $P = 0.26 \pm 0.24$  per cent), has a position angle of  $175^\circ$  and a large error bar ( $\pm 26^\circ$ ) associated with the measurement. It can be seen from Fig. 2 that stars (1, 2, 5, 11) seen projected outside the nebular cloud boundaries (Fig. 1), and other stars (6, 9, 10, 13, 16) showing low values of polarization ( $\leq 0.34$  per cent) exhibit a large dispersion ( $\sigma_\theta = 39^\circ$ ) in position angles around a mean  $\langle \theta \rangle = 106^\circ$ . These stars may be suffering only small values of polarization as a result of the low-density interstellar medium outside of the cloud or foreground to it. Stars (3, 4, 7, 8, 12, 14, 15) showing larger ( $> 0.34$  per cent) values of polarization are characterized by a position-angle distribution with a mean  $\langle \theta \rangle = 77^\circ$  and a relatively smaller dispersion  $\sigma_\theta = 19^\circ$ . These stars are likely to be background stars,

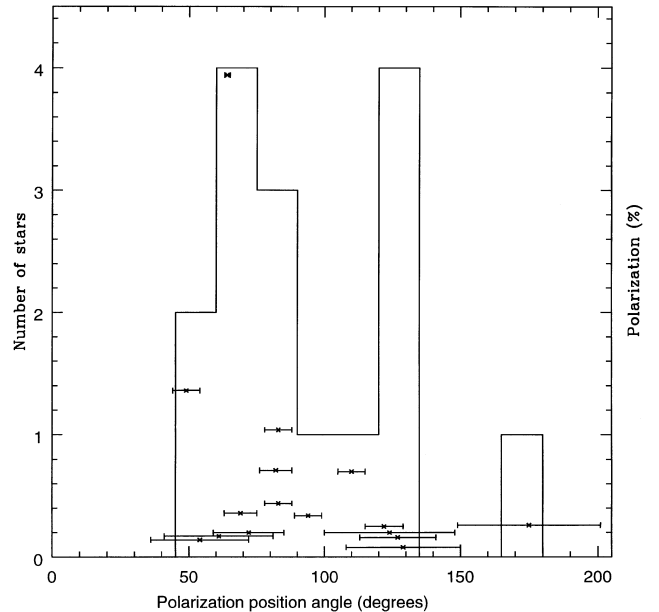


**Figure 2.** Histogram showing the distribution of the observed polarization position angles for stars in the region of CG 30–31. The measured percentage polarization (with the scale on the right) for the stars is indicated by the symbol \*.

their light being polarized by aligned dust grains in the clouds associated with the CG 30–31 complex.

If the polarization is caused by dust grains aligned by the magnetic field (Davis–Greenstein mechanism), then the polarization vectors drawn in Fig. 1 are also parallel to the projected direction of the magnetic field in the region. The observed distribution of position angles therefore can be interpreted as follows. The magnetic field in the CG 30–31 cloud complex is more or less unidirectional with a projected position angle  $\sim 77^\circ$ . This is because the dispersion in the position angles for stars that have larger values of polarization (caused mainly by the dust in the cloud that has a small spatial extent  $\sim 2$  pc) is relatively small ( $\sigma_\theta = 19^\circ$ ). For stars with low values of polarization, the distribution of position angles is determined by the magnetic field over a longer path-length ( $\sim 400$  pc) in the lower-density interstellar medium. Changes in the field direction over the longer

path-length could cause the larger dispersion in the observed polarization position angles for these stars.

It would be interesting to see if one could find other independent ways to discriminate between stars foreground to the cloud and those background to it. The most direct method is the measurement of trigonometric parallaxes. The *Hipparcos* astrometry satellite has recently provided a data base of such measurements in the form of the *Hipparcos* and *Tycho* catalogues (ESA 1997). Unfortunately none of the stars observed here have accurate parallax measurements in the *Hipparcos* catalogue. However, one of the low-polarization stars (star 6  $\equiv$  SAO 198851) is listed in the *Tycho* catalogue (which gives less precise astrometric measurements) to have a parallax  $\pi = 28.8 \pm 14.0$  mas. The most probable distance ( $d$ ) to star 6 is thus  $\sim 35$  pc. This supports the classification of this star as a star foreground to the CG 30–31 cloud complex ( $d \sim 415$  pc).

A correlation between the measured percentage polarization  $P$  and the reddening [colour excess  $E(B - V)$ ] for the stars is also expected if dust is the cause of extinction and polarization. However, the colour excess can be estimated only for two of our programme stars (1 and 5) as the spectral types and photometry are not available for the other stars. For stars 1 (SAO 198864) and 5 (SAO 198868) we find, from the SIMBAD data base at CDS, Strasbourg, spectral types and  $B, V$  photometric magnitudes given as: B8–9/III–IV,  $B = 9.6$ ,  $V = 9.7$  (star 1); G6III,  $B = 9.0$ ,  $V = 8.1$  (star 5). With standard intrinsic colours  $(B - V)_i \approx -0.1$  for star 1 and  $\approx 0.9$  for star 5, and absolute magnitudes  $M_V \approx -0.6$  for star 1 and  $\approx 1.2$  for star 5 corresponding to their respective spectral types from Schmidt-Kaler (1965), we estimate the values of colour excesses  $E(B - V)$  and distance moduli  $\Delta m = (V - M_V)$  for these stars given by:  $E(B - V) \approx 0.0$ ,  $\Delta m \sim 10.3$  ( $d \sim 1150$  pc) for star 1 and  $E(B - V) \approx 0.0$ ,  $\Delta m \sim 6.9$  ( $d \sim 240$  pc) for star 5. There could be some uncertainties in the spectral class (say one subclass) and also in the photometric magnitudes (say  $\sim 0.1$  mag), but it is unlikely that stars 1 and 5 have any significant colour excesses  $E(B - V)$  much larger than  $\sim 0.1$  mag. Their observed polarizations are also low. While star 5 is a nearby star closer to us than the CG complex, star 1 is a more distant star. Both are seen projected outside the cloud boundaries.

The observed distribution of polarization values and position angles suggests that the projected magnetic field in the CG 30–31 cloud complex is oriented in the direction  $\theta = 77^\circ \pm 19^\circ$ . The relative orientations of the magnetic field and the cometary tails in CG 30–31 are quite different. The position angles for the CG tails are  $\sim 165^\circ$  (Zealey et al. 1983), whereas the mean position angle for the magnetic field in CG 30–31 is  $\sim 77^\circ$ . Thus the magnetic field is nearly perpendicular to the CG tails. This is unlike the case for CG 22 (Paper I) in which the field is oriented parallel to the tail.

A magnetic field oriented parallel to the CG tail could help confine the tail in the direction normal to the field. This is perhaps so in CG 22 (Paper I). CG 22 has a very long, well-formed tail. Its head is of size  $3 \times 5$  arcmin, while the tail length is 74 arcmin. The ratio of tail length to head size (aspect ratio) for the cometary tail of CG 22 is  $\sim 15$ , the largest value observed for any CG. In the absence of any confining forces, the observed gas velocity dispersion ( $\sim 1 \text{ km s}^{-1}$ ) in the CG tail would lead to dispersal of cloud gas in the direction perpendicular to the tail. This is prevented by a magnetic field oriented parallel to the tail in CG 22. The cometary tails in the CG 30–31 complex are much shorter and appear to form a rather amorphous mass behind the CG heads. The magnetic field is observed to be oriented perpendicular to the tails. Such a field geometry may restrict the formation of long tails

and permit dispersal of cloud gas parallel to the field (perpendicular to the tails). The morphology of the CGs may thus depend on the relative orientation of the magnetic field in the globules with respect to the radius vector from the central source of radiation and stellar winds (that cause the formation of the CGs) and the globule head. If the field happens to be parallel to the radius vector, then conditions are favourable for the formation of a narrow, long tail. For other relative orientations of the magnetic field, shorter tails with smaller aspect ratio are produced. Observations of other CGs located at different positions in the Vela–Puppis complex help clarify the relation between CG morphology and the magnetic field geometry in the globules.

A bipolar molecular outflow associated with CG 30 has been recently detected by Nielsen et al. (1998). The outflow originates from IRS 4 and drives the Herbig–Haro object HH 120. It is interesting to note that Nielsen et al. (1998) found the molecular outflow to be directed perpendicular to the tail of CG 30. The outflow is thus more or less parallel to the magnetic field in the cloud. This is consistent with the current theories of star formation which suggest the formation of flattened circumstellar structures perpendicular to the magnetic field and molecular outflows channelled along the field.

## 6 CONCLUSIONS

Polarization measurements of stars in the region of the cometary globules CG 30–31 in Vela–Puppis have been used to map the geometry of the magnetic field in this CG complex. The magnetic field in the cloud is found to be oriented nearly perpendicular to the cometary tails of the CGs. This is in contrast with the situation in CG 22, where the field is parallel to the tail. It is suggested that the CG morphology depends on the relative orientations of the cloud magnetic field and the radius vector of the CG head from the central source of radiation and winds that produce the cometary tails. Long, narrow tails result when the magnetic field is parallel to the radius vector. For a cloud magnetic field that is perpendicular to the driving force, the gas flow along the tail is inhibited, resulting in a shorter and more diffuse tail.

The cloud magnetic field is nearly parallel to the molecular bipolar flow associated with young stellar object IRS 4 embedded in the head of CG 30. This is consistent with current theories of star formation that suggest cloud collapse parallel to the magnetic field, leading to the formation of a flattened disc perpendicular to the field and a bipolar flow channelled parallel to the field.

## ACKNOWLEDGMENTS

I thank the referee, Prof. W. J. Zealey, for comments that led to a number of clarifications. Swara Ravindranath is thanked for her help in the preparation of Fig. 1. This research has made use of the SIMBAD data base, operated at CDS, Strasbourg, France. The optical image in Fig. 1, reproduced from the Digitized Sky Survey, is based on photographic data obtained using the UK Schmidt Telescope operated by the Royal Observatory Edinburgh, with funding from the UK Science and Engineering Research Council and the Anglo-Australian Observatory. The Digitized Sky Survey was produced at the Space Telescope Science Institute under the US Government grant NAG W-2166.

## REFERENCES

Bertoldi F., 1989, *ApJ*, 346, 735

- Bertoldi F., McKee C. F., 1990, *ApJ*, 354, 529  
Bhatt H. C., 1993, *MNRAS*, 262, 812  
Block D. L., 1992, *ApJ*, 390, L13  
Brand P. W. J. L., Hawarden T. G., Longmore A. J., Williams P. M., Caldwell J. A. R., 1983, *MNRAS*, 203, 215  
Brandt J. C., Stecher T. P., Crawford D. L., Maran S. P., 1971, *ApJ*, 163, L99  
de Zeeuw P. T., Brown A. G. A., de Bruijne J. H. J., Hoogerwerf R., Lub J., Le Poole R. S., Blaauw A., 1997, *ESA SP-402*, 495  
ESA, 1997, *The Hipparcos and Tycho catalogues. ESA SP-1200*  
Gum C. S., 1952, *Observatory*, 72, 151  
Gyulbudagyan A. L., 1985, *AFz*, 23, 295  
Hawarden T. G., Brand P. W. J. L., 1976, *MNRAS*, 175, 19P  
Hsu J. C., Breger M., 1982, *ApJ*, 262, 732  
Jain S. K., Srinivasulu G., 1991, *Opt. Eng.*, 30, 1415  
Lefloch B., Lazareff B., 1994, *A&A*, 289, 559  
Lefloch B., Lazareff B., 1995, *A&A*, 301, 522  
Nielsen A. S., Olberg M., Knude J., Booth R. S., 1998, *A&A*, 336, 329  
Pettersson B., 1984, *A&A*, 139, 135  
Reipurth B., 1981, *A&AS*, 44, 379  
Reipurth B., 1983, *A&A*, 117, 183  
Sahu M. S., 1992, PhD thesis, Univ. Groningen  
Sandqvist Aa., 1976, *MNRAS*, 177, 69P  
Scarrott S. M., Gledhill T. M., Rolph C. D., Wolstencroft R. D., 1990, *MNRAS*, 242, 419  
Schaerer D., Schmutz W., Grenon M., 1997, *ApJ*, 484, L153  
Schmidt-Kaler Th., 1965, in Voigt H. H., ed., *Landolt-Bornstein, Vol. I, Astron. and Astrophys. Group VI*. Springer-Verlag, Berlin, p. 298  
Schneps M. H., Ho P. T. P., Barret A. H., 1980, *ApJ*, 240, 84  
Serkowski K., 1974, in Gehrels T., ed., *Planets, Stars and Nebulae studied with Photopolarimetry*. Univ. of Arizona Press, Tucson, p. 135  
Sridharan T. K., 1992, *JA&A*, 13, 217  
Sridharan T. K., Bhatt H. C., Rajagopal J., 1996, *MNRAS*, 279, 1191 (Paper I)  
Sugitani K., Fukui Y., Ogura K., 1991, *ApJS*, 77, 59  
Zealey W. J., Ninkov Z., Rice E., Hartley M., Tritton S. B., 1983, *Astrophys. Lett.*, 23, 119

This paper has been typeset from a  $\text{\TeX}/\text{\LaTeX}$  file prepared by the author.